USDA
United States Department of Agriculture

GTAC-10211-RPT1 July 2020

Mapping Sudden Oak Death in Southwest Oregon

Credit: Photo courtesy of Sarah Navarro

Non-Discrimination Policy

The U.S. Department of Agriculture (USDA) prohibits discrimination against its customers, employees, and applicants for employment on the bases of race, color, national origin, age, disability, sex, gender identity, religion, reprisal, and where applicable, political beliefs, marital status, familial or parental status, sexual orientation, or whether all or part of an individual's income is derived from any public assistance program, or protected genetic information in employment or in any program or activity conducted or funded by the Department. (Not all prohibited bases will apply to all programs and/or employment activities.)

To File an Employment Complaint

If you wish to file an employment complaint, you must contact your agency's EEO Counselor within 45 days of the date of the alleged discriminatory act, event, or personnel action. *Additional information can be found online at http://www.ascr.usda.gov/complaint_filing_file.html.

To File a Program Complaint

If you wish to file a Civil Rights program complaint of discrimination, complete the USDA Program Discrimination Complaint Form, found online at http://www.ascr.usda.gov/complaint_filing_cust.html, or at any USDA office, or call (866) 632-9992 to request the form. You may also write a letter containing all of the information requested in the form. Send your completed complaint form or letter to us by mail at U.S. Department of Agriculture, Director, Office of Adjudication, 1400 Independence Avenue, S.W., Washington, D.C. 20250-9410, by fax (202) 690-7442 or email at program.intake@usda.gov.

Persons with Disabilities

Individuals who are deaf, hard of hearing or have speech disabilities and who wish to file either an EEO or program complaint please contact USDA through the Federal Relay Service at (800) 877-8339 or (800) 845-6136 (in Spanish).

Persons with disabilities who wish to file a program complaint, please see information above on how to contact us by mail directly or by email. If you require alternative means of communication for program information (e.g., Braille, large print, audiotape, etc.) please contact USDA's TARGET Center at (202) 720-2600 (voice and TDD).

Rounds, E.; Olimpio, B.; Schaaf, A.; Fisk, H.; Davenport, J. 2020. Mapping sudden oak death in southwestern Oregon. GTAC-10211-RPT1. Salt Lake City, UT: U.S. Department of Agriculture, Forest Service, Geospatial Technology and Applications Center. 28 p.

Abstract

Sudden oak death (SOD) is caused by an invasive pathogen, *Phytophthora ramorum* (*P. ramorum*), that has been killing tanoak trees in southwestern Oregon since 2001. Tanoak is an ecologically important keystone species that is the only acorn producer in its range, and it has high cultural value for the Native American tribes in the region. After initial attempts to eradicate the pathogen proved unsuccessful, land managers transitioned to a containment strategy that focused on limiting the spread of SOD. A critical part of this containment strategy is being able to quickly identify new outbreaks. Since 2012, the Oregon Department of Forestry has acquired annual high resolution (30 cm), 4-band multispectral airborne imagery to quantify and monitor disease spread and intensification. Current methods that rely on photointerpretation and manual delineation to assess SOD are inefficient and non-exhaustive.

This project investigated whether Structure from Motion (SfM) workflows could be used to characterize the structure of infected tanoak trees and detect changes in canopy morphology over time. Supervised image classification methods were also tested to see if tanoak trees potentially infected with *P. ramorum* could be detected over large areas in a semi-automated process. Findings showed that the high-resolution imagery available in the southwestern Oregon study area were not collected with the overlap necessary for SfM workflows, and the resulting data products were not sufficient for characterizing tanoak canopies. Moreover, supervised classification methods were unable to accurately differentiate dead tanoak from other dead species, and the bare ground was commonly confused with dead trees in classification outputs. The resulting classified products, however, could be used in conjunction with image mosaics to guide image interpretation efforts aimed at identifying dead and dying tanoaks.

Authors

Eric Rounds is a Remote Sensing Specialist and trainer employed by RedCastle Resources, Inc., at the Geospatial Technology & Applications Center (GTAC) in Salt Lake City, UT.

Ben Olimpio is a Geospatial Programmer employed by RedCastle Resources, Inc., at GTAC in Salt Lake City, UT.

Abigail Schaaf is a Remote Sensing Project Manager employed by RedCastle Resources, Inc., at GTAC in Salt Lake City, UT.

Haans Fisk is the program leader for the Resource Applications and Technology Implementation (RATI) program at GTAC in Salt Lake City, UT.

Julie Davenport is a Photogrammetry and Lidar Specialist for the Resource Applications and Technology Implementation (RATI) program at GTAC in Salt Lake City, UT.

Table of Contents

Introduction

Sudden oak death (SOD) is caused by an invasive pathogen, *Phytophthora ramorum* (*P. ramorum*), that has been aggressively killing tanoak trees in southwestern Oregon since 2001 (Goheen and others, 2002) and northern California since 1995 (Garbelotto and others, 2001). Tanoak is an ecologically important keystone species that is the only acorn producer in its range, and it has high cultural value for the Native American tribes in the region. *P. ramorum* spores spread from infected foliage by means of wind and wind-driven rain. Spores penetrate into the bark of tanoaks where they then colonize the tissue, creating cankers in the bole (Figure 1) that cut off the flow of nutrients and water, effectively girdling the tree and likely killing it (Grünwald and others, 2012). Federal and state agencies have partnered with private landowners to facilitate the survey, detection, and eradication of SOD. Areas infected with SOD have been managed through the designation of a SOD Quarantine Area (Figure 2) under the authorities of the Oregon Department of Agriculture (ODA) and U.S Department of Agriculture (USDA) Animal Plant Health Inspection Service. However, because eradication efforts failed to stop the spread of the pathogen, Oregon's disease management program transitioned in 2012 from an effort to eradicate to one focused on slowing the spread of the pathogen (Goheen and others, 2017).

Figure 1: Image of dead or dying tanoak (left) and an image of a canker in a tanoak (right)

In order to monitor and limit the spread of SOD, land managers depend on accurate spatial data on the location of new outbreaks. When SOD was first detected in Oregon, land managers started performing aerial surveys in southwest Oregon to detect and digitize dead or dying tanoaks and other tree species killed by *P. ramorum*. Beginning in 2012, the Oregon Department of Forestry (ODF) started contracting the annual acquisition of high-resolution aerial imagery over the Quarantine Area in southwestern Oregon. Forest pathologists and field technicians manually scan the imagery and digitize potential dead

or dying tanoak before visiting those locations in the field to collect samples, which are then tested for the presence of *P. ramorum*. They do this iteratively, scanning the imagery again for new infestations each time before returning to the field to collect samples. Efforts to limit spread and eradicate new infestations largely consist of a combination of cutting down host plants in and around infected areas (e.g., tanoak, rhododendron, huckleberry and Oregon myrtle), applying herbicides to reduce the sprouting of infected host plants, and the subsequent burning of felled plants (Goheen 2006; Hansen and others, 2019).

The current manual delineation methods that ODF employ to track the spread of SOD are labor intensive, non-exhaustive and imprecise. Moreover, ODF and the USFS wanted to evaluate more novel remote sensing methods for identifying changes in canopy structure (e.g., shrinking crown diameter) from year to year that could be an early onset symptom of infected trees. For this project funded by the Geospatial Technology and Applications Steering Committee (GeoTASC), remote sensing specialists from the USDA Forest Service (USFS) Geospatial Technology and Applications Center (GTAC) partnered with experts from ODF and the Pacific Northwest Region of the USFS to identify suitable remote sensing workflows for detecting trees potentially infected with *P. ramorum*. The primary objectives of this project were 1) to test remote sensing workflows that could increase the efficiency with which potential SOD outbreaks are detected, as well as to identify annual spread of SOD and 2) test Structure from Motion (SfM) workflows for generating high quality, three-dimensional (3D) point clouds. Ideally, these efforts would provide accurate spatial information on dead tanoak locations for each year of available imagery, and the SfM outputs would provide structural information on the canopies that could be used to detect early onset symptoms of SOD that were potentially unrelated to spectral characteristics.

Methods

Study Area

The SOD Quarantine Area is a 514 square mile area located in southwestern Oregon (Figure 2), west of the Cascade Range and adjacent to the Rogue River-Siskiyou National Forest. The Quarantine Area boundary is where land managers expect to be able to contain the spread of SOD through management actions. The environment is characterized by a mixture of coastal and rugged mountainous terrain, with vegetation that is a mixture of deciduous and conifer, open and closed canopy, with low shrubs along riparian corridors. The majority of land within the Quarantine Area is privately owned, with much of it owned by timber companies. The Generally Infested Area (GIA) was established in 2013 around the densest concentration of the SOD outbreak where eradication efforts were no longer required so that available funding could be prioritized in areas closer to the Quarantine boundaries (Goheen and others, 2017). The southern extent of the Generally Infested Area (GIA) is approximately 4 miles north of California, with the western extent following the Oregon coast. To keep file sizes manageable and to reduce processing times, we tested remote sensing workflows on a 30 square mile project area of interest (AOI) in the northern part of the Quarantine Area by Gold Beach, OR.

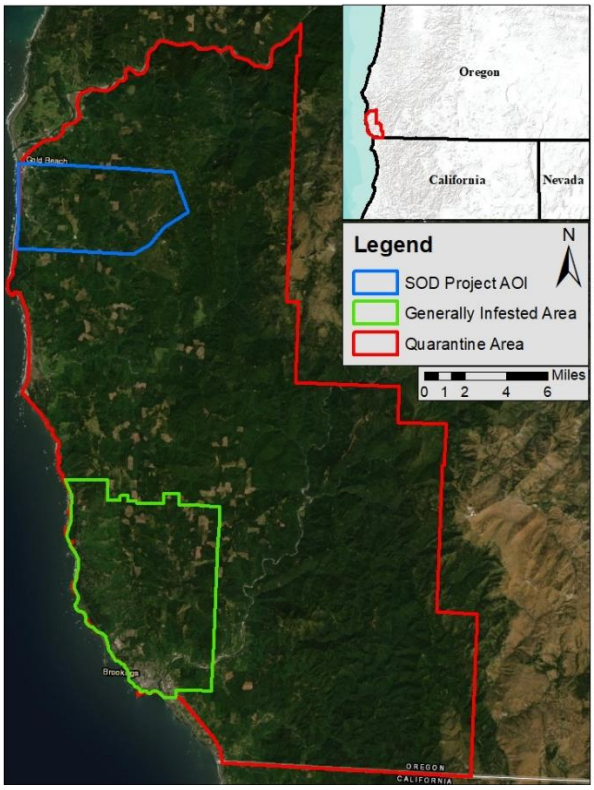

Figure 2: Map of SOD Quarantine Area, Generally Infested Area and Project AOI in Southwestern Oregon.

Annual Aerial Imagery

High resolution (30cm) color-Infrared (CIR) imagery is collected annually for the SOD Quarantine Area. The vendor delivers individual images in TIFF or IMG format depending on the year, as well as mosaic datasets for each year. Each image and mosaic have four bands: Blue, Green, Red, and Near-Infrared, and have a pixel resolution of one foot. ODF provided GTAC with imagery for 2012-2017 and 2019.

Upon inspection, we identified issues with the individual images and mosaic datasets. The primary issue was that there were black areas around each individual image (figure 3) that had values of 0 for each band instead of the NoData values they should have had. This is problematic for creating image mosaics because the standard mosaic operators would either include the black areas around the image in the resulting mosaic or create a blurred image in areas where the images overlap. When looking at the mosaics that were provided, like in Figure 3, there were noticeable areas within the image that were blurry and we could not visually identify the features.

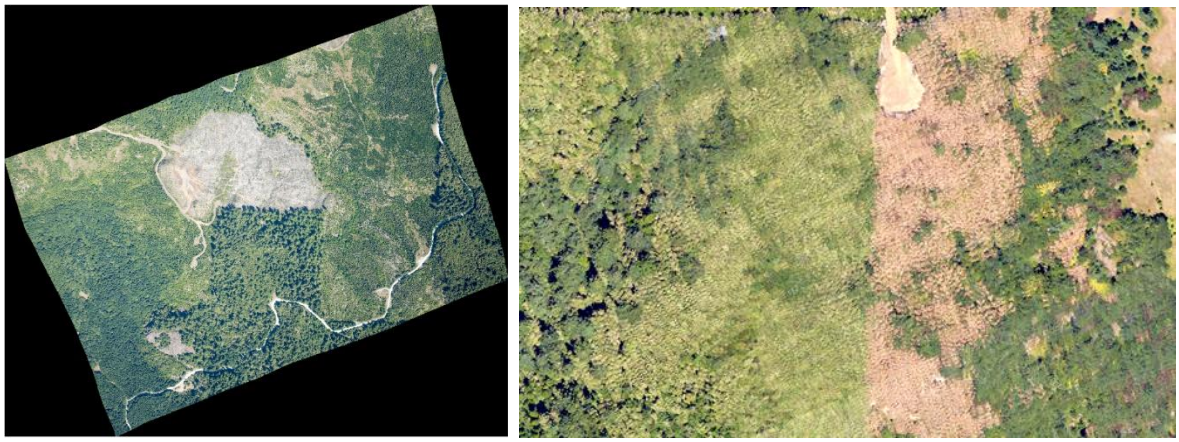

Figure 3: Example of the blurry vendor-supplied mosaics.

To address these issues with both the individual images and the mosaics, we developed a Python script that first masks out all the areas in each image that have zero values for all four bands and then mosaics the fixed imagery together using the "last" mosaic operator option to create an improved mosaic.

Another issue with the aerial imagery was that only the orthocorrected images were delivered by the vendor, and they were therefore not suitable for SfM testing, which requires non-orthocorrected imagery and flight metadata with locational information for each image. Since this data was not initially delivered by the vendor, ODF purchased the additional, non-orthocorrected data to be used in this project. The vendor delivered this data for 5 years ('13, '15-'17, and '19) with accompanying text files for each year that provide the necessary flight metadata for each image.

In addition to the annual imagery, ODF provided manually digitized tanoak mortality polygons that, when overlaid on the imagery, were useful for informing image interpretation and training data collection. While point shapefiles were provided that represent the GPS location of positive SOD samples, the spatial accuracy of the points was poor, meaning they couldn't be used as training data because they didn't align closely enough with imagery.

Structure from Motion

SfM is a method by which dense 3D point clouds are derived from overlapping aerial imagery using semi-automated stereoscopic techniques (Verhoeven 2011). For this project, we used Agisoft Metashape software (version 1.5.5) to test the suitability of the aerial imagery for SfM workflows. Ideally, the 3D point cloud outputs would enable us to produce detailed raster derivatives that capture the nuances of canopy surfaces in the study area. Panagiotidis and others (2017) demonstrated the application of SfM techniques for producing canopy height data and subsequent individual tree segments that can be used to estimate crown dimensions. Burnett and others (2017) used a similar approach, but they took it a step further by using individual tree segments and the imagery it was derived from to classify a Swiss needle cast outbreak in northwest Oregon. That data, however, was created from 2.5 cm UAS imagery, which is a much finer resolution than our available imagery. Even so, with multiple years of data, we could potentially identify early symptoms of SOD unrelated to changes in color, such as a reduction of crown size.

Certain acquisition specifications are key to the production of high-quality SfM products. Most importantly, stereo pairs should have 80% endlap and 60% sidelap, as this will result in fewer holes and shadowed areas in the point cloud, along with more observations at nadir. This is especially important in forested environments where adjacent images captured from closer viewpoints will facilitate more successful matching of adjacent images due to the similar appearance of features in both images (Webb and others, 2017; Westoby and others, 2012). Another key consideration for SfM workflows is the availability of high-resolution digital terrain models (DTM). An accurate DTM is critical for generating a canopy height model (CHM), which is a digital surface model (DSM) normalized to above ground heights. In areas where there is very sparse vegetation, it is possible to create a relatively accurate DTM from the aerial imagery using SfM. However, in densely forested environments where the bare earth surface is consistently obscured, having a lidar- derived DTM is ideal (Webb and others, 2017; Wallace and others, 2016). The imagery available for this project was not acquired with the recommended overlap specifications, and it therefore may not be suitable for creating high quality products due to the relatively limited overlap. Moreover, a high-resolution lidar-derived DTM is only available for the western portion of the AOI, while a 10 ft. DTM is available for the eastern portion. This will have a negative impact on the quality of the CHM for the eastern part of the AOI.

Classification

The primary way that we attempted to detect SOD was by performing supervised classifications. Supervised classification is a commonly used image classification technique that relies on the input of land cover samples and their spectral characteristics to predict wall-to-wall land cover types. For this project, we explored three classification methods, two of which require classification schemes. The Support Vector Machine (SVM) and Maximum Likelihood Classification (MLC) algorithms, which are available in ArcGIS Pro (version 2.5), require a defined classification scheme for the algorithms to know how to classify an image. Classification schemes must include unique, mutually exclusive land cover classes that capture the full variation of land cover in the study area. For this project, we decided upon the classification scheme outlined in table 1. Because we knew it was difficult to separate dead grey tanoak from other dead grey tree species, we decided to add the Recently Dead Tanoak class, which appears as a reddish-brown tanoak that likely died within the previous two years. The third classification that we tested was Maximum Entropy (MaxEnt), which was attractive because it only requires samples from a single class of interest (Phillips and others, 2017).

Once the classification scheme was finalized, we created the classification training points used to train the classification algorithms in ArcGIS Pro. Having accurate training data is crucial to the classification process because both the SVM and the MLC classification algorithms use the spectral signatures of each training point to train the classifier. We also use a subset of these classification points to perform error analysis on the classification output.

Table 1: Class Names and Values

Class name	Class value
Live Deciduous Trees	1
Live Coniferous Trees	2
Bare Ground	3

Roads	4
Buildings	5
Water	6
Recently Dead Tanoak	7
Other Dead	8
Old Dead Tanoak	9

Training Data Creation for Classification and Accuracy Assessment

To create the training dataset, we interpreted the aerial imagery in ArcGIS Pro to identify examples of each land cover type. Once examples were identified, we placed a point in each location and updated the attribute table with the corresponding land cover class names and values. For the 2019 SVM and MLC classifications, there were 500 total points interpreted for the classification. 30% of those points (150 points) were withheld from the classification in order to perform an accuracy assessment on the classification outputs. The accuracy dataset was created by generating an evenly weighted, random subset of points within ArcGIS Pro. Once each classification iteration was complete, the classified images were sampled at each of the accuracy assessment points in order to compare the predicted class with the reference class. From this information we generated an estimate of overall accuracy of the classified image as well as the accuracy for each class. This is done by creating error matrices that break down the number of correctly and incorrectly classified pixels by each land cover class. Since the goal of the 2017 MLC was to assess the feasibility of using the signature file from the 2019 MLC training data, we only needed to interpret points for the accuracy assessment. A total of 90 points were interpreted for the 2017 MLC accuracy assessment.

Support Vector Machine

The first classification algorithm that we tested was ArcGIS Pro's Support Vector Machine. SVM attempts to identify patterns, both spectral and non-spectral, from multi-spectral imagery using statistical decision making to create a classified image (Oommen and others, 2008). An important characteristic of this classification algorithm in ArcGIS Pro is that it is object-based. Object-based classification approaches rely on a segmented image, which is created by grouping adjacent pixels together based on their similar spectral characteristics. For this project, we used the Segmentation tool in ArcGIS Pro to segment the four-band imagery mosaic by applying user-defined spectral and spatial weights. An example of a segmented image is shown in Figure 4. Once the segments are created, the mean spectral value for each segment is calculated and the value is extracted to overlapping training data points. The training data and image are then ingested into the SVM tool.

Figure 4: Segmented image (right) compared to the actual image (left). The segmented image groups pixels with similar spectral characteristics, with the value for each segment representing the mean value of those pixels.

Maximum Likelihood Classification

Another classification algorithm that we used to try to detect dead tanoak in the study area was the MLC. In contrast to the SVM algorithm, the MLC algorithm is pixel-based, meaning that it only relies on the spectral signature of a given pixel to classify the image. MLC executes this classification by using a signature file that is created from training data. Because the classification algorithm is pixel-based, it is simple to add more data layers (e.g., a DSM or a NDVI layer) that may improve class separability. We added the Normalized Difference Vegetation Index (NDVI) layer to the input classification bands. The NDVI is a simple differencing between the Near-Infrared (NIR) and the Red bands of the image (see equation 1), and it has values ranging from -1 to 1, with higher values signifying the presence of healthy, green vegetation.

$$NDVI = \frac{(NIR - Red)}{(NIR + Red)}$$

Equation 1. The Normalized Difference Vegetation Index

The NDVI for each year's imagery in this project was added as additional input to help differentiate between some of the non-vegetation and vegetation classes that had similar spectral signatures. The signature file was created from the most recent imagery (2019) and was applied to both 2017 and 2019 imagery. If successful, this approach would be advantageous because a new training dataset would not need to be created every year, thus improving efficiency of SOD detection.

Maximum Entropy Classification

The last classification approach that we tested was the MaxEnt classification. This classification originated from species modeling in biology and seemed promising because it only classifies one target class at a time using a series of empirical formulas. This is particularly attractive since the only class we are interested in is Recently Dead Tanoak. We used an open source MaxEnt program developed by the

American Museum of Natural History through a collaboration with AT&T-research (Phillips and others, 2017).

This program has a plethora of parameters that can customized for any model run (Figure 5), but due to time constraints, this project used the default values. Before running this program, input imagery also must be converted to an ASCII file format. We ran two iterations of this algorithm on two different training datasets: Recently Dead Tanoak and Other Dead trees. As input to the program, we supplied the training points for the target class, along with the multispectral ASCII mosaic for 2019.

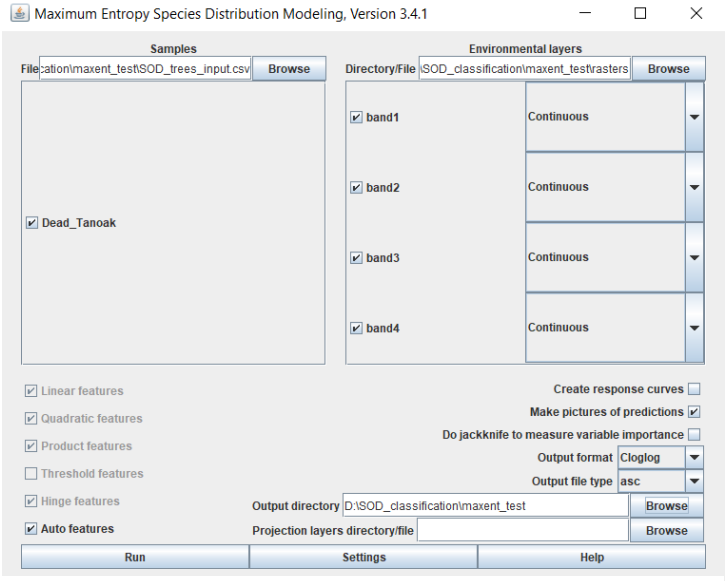

Figure 5: MaxEnt model dialogue with desired inputs

Results

Structure from Motion

There were several outputs from the SfM processing, including the dense point cloud, DSM, and CHM. Figure 6 is an oblique view of the colorized point cloud displayed in Metashape. The lighter colored trees are largely tanoak, while the darker colored trees are mostly Douglas fir. The grey areas, which are particularly noticeable at the bottom of the image, are NoData areas that are a result of the overlapping imagery not capturing a complete view of vegetation from multiple angles. Another thing to notice is the relatively limited detail in the tanoak stands, which appear to have high canopy cover and similar heights, resulting in a relatively smooth looking canopy surface. The limited amount of detail in the canopy surface and the widespread areas of NoData indicate a lack of overlap in the imagery used to perform the SfM process. With a greater amount of endlap and sidelap in the input imagery, these data voids would be much less widespread and the dimensions of individual trees would be better represented in the point cloud and resulting products.

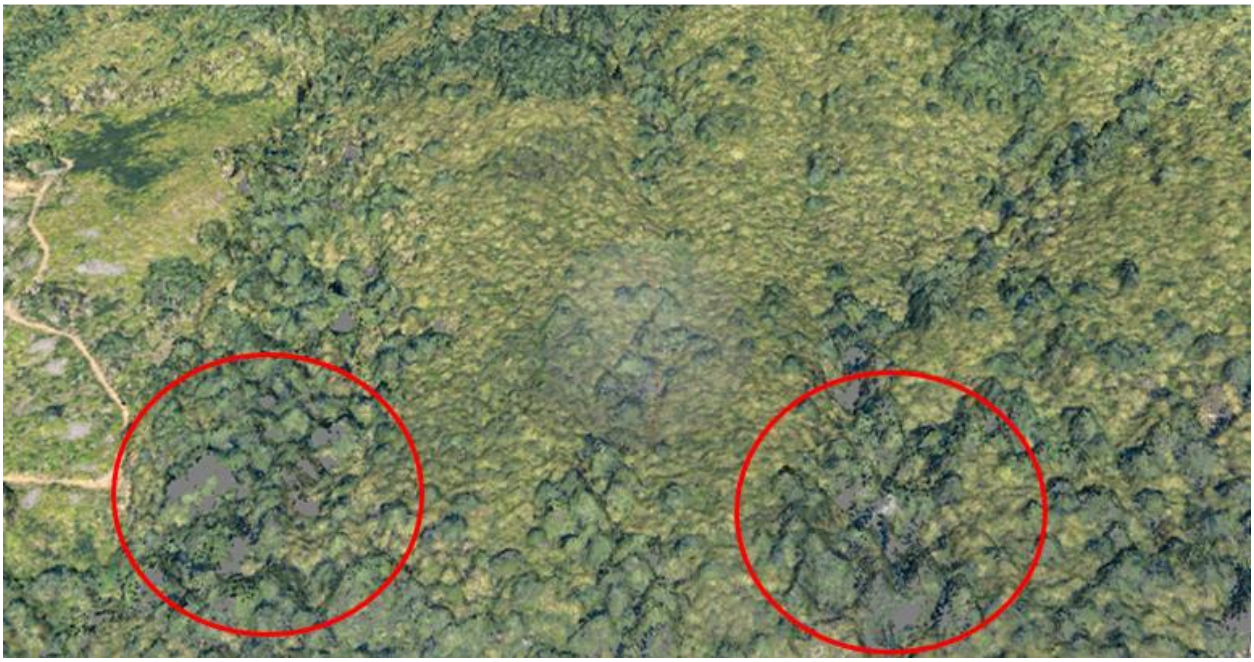

Figure 6: Oblique view of SfM-derived point cloud displayed in Metashape.

We derived CHMs to test whether we could differentiate between individual canopies and create an accurate canopy/non-canopy mask. Figure 7 shows the DSM and CHM results derived from an area in the eastern part of the AOI, where only a 10 ft. DEM was available to normalize DSM values to above ground heights. Figure 8 shows the same thing but in an area in the western part of the AOI where a 3 ft. lidar-derived DEM is available. The lower quality of figure 7 is exemplified by the coarser resolution of the CHM output as well as the lower level of detail that is apparent in the forested areas. In figure 8, changes in canopy height from tree to tree are much easier to identify than in figure 7. The errors in the CHM values in both figures are apparent, however. Figure 7 has a low canopy height value of -56 ft., while figure 8 has a low canopy height value of -11. This suggests errors in the production of the DSM, as each of the CHMs should have a minimum value of 0 when there is bare ground in the display extent.

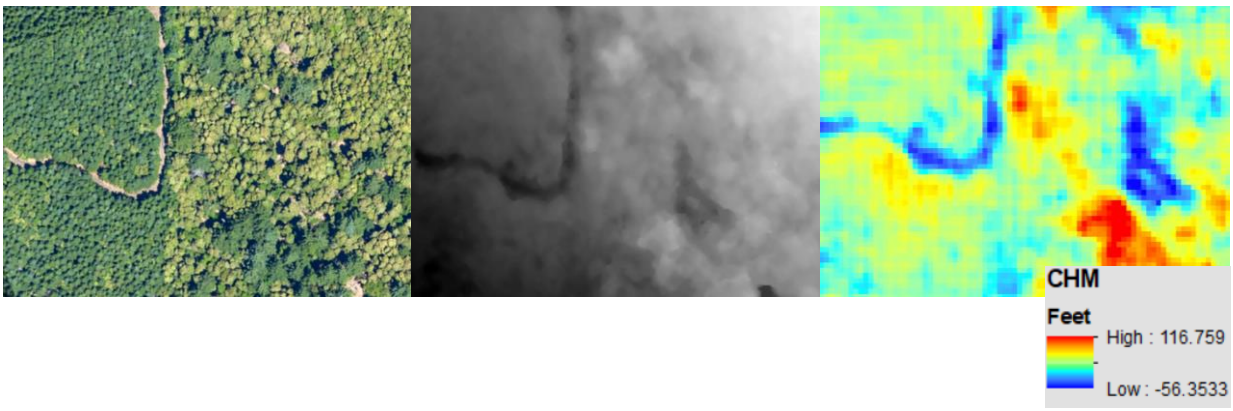

Figure 7: 2019 Imagery (left), SfM-derived DSM (center), CHM (right); color ramp represents low to high elevations (blue to red).

Figure 8: 2019 Imagery (left), SfM-derived DSM (center), CHM (right); color ramp represents low to high elevations (blue to red)

Creation of new mosaics

The python script developed for this project successfully creates mosaics without blur by identifying and clipping out areas in the individual images that should be NoData and then mosaicking all the resulting images for each year. New mosaics were created for each year that data was available. Figure 9 shows the difference between the vendor-delivered mosaics and the new mosaics. In the image on the left of Figure 9, features are indiscernible due to the blur effect. However, in the image on the right, it is much clearer, making the image suitable for classification.

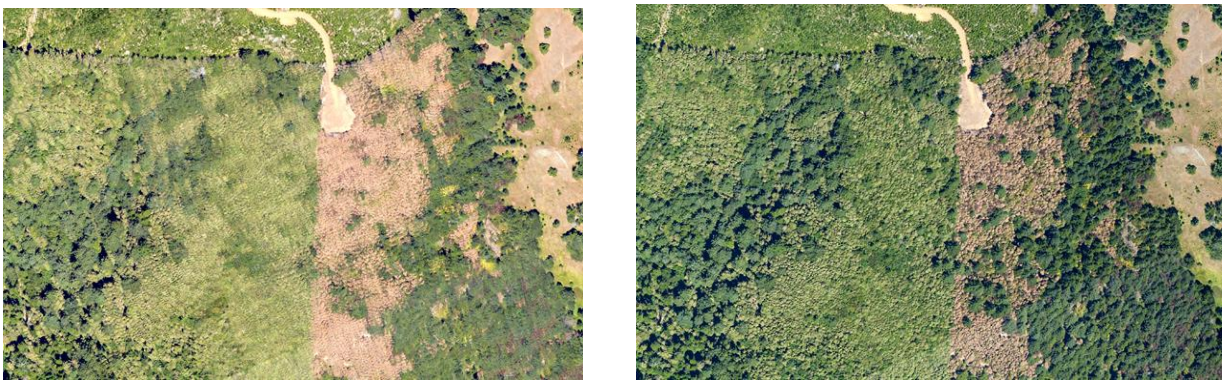

Figure 9: Comparison between the vendor supplied mosaic (left) and the new mosaic created for this project (right).

Classification results

Support Vector Machine

Part of the SVM testing required the identification of the ideal segmentation parameters. We tested several different combinations of the input weights (spectral, spatial, minimum segment size) to identify the best parameters for the SVM classification, the results of which are attached in Appendix A. The parameters that were ultimately selected are as follows: spectral weight set to the maximum value, 20; spatial weight set to 15; minimum segment size set to 75 pixels. Figure 10 shows some of the segments (yellow polygons) that overlap with Recently Dead Tanoak training data (green dots), the spectral values for which were used as input to the SVM tool. Figure 11 shows a subset of the 2019 SVM classification results, along with the corresponding imagery and a legend showing which class each color represents.

Figure 10: Example of segments (yellow) that overlap with training data (light green dots).

Figure 11: 2019 unclassified image (left) and the 2019 SVM classified image (right).

Table 2: Errors summarized for each of the classes for the 2019 SVM classification.

SVM 2019 classes	Error of Omission (%)	Error of Commission (%)
Live Deciduous	8	0
Live Coniferous	10	18
Bare Ground	9	33
Roads	6	21
Buildings	60	33
Water	0	0
Recently Dead Tanoak	8	3
Other Dead	21	19
Old Dead Tanoak	29	29
	Total Accuracy (%)	85

Table 2 shows the errors of omission and commission for the 2019 SVM results. The full error matrix is available in Appendix B. The overall accuracy of the SVM results was 85%. The Other Dead and Old Dead Tanoak classes had errors of omission (21% and 29%, respectively) and of commission (19% and 29%, respectively), which is relatively high but to be expected with two classes that are spectrally similar. The error matrix suggests that there were few errors in the prediction of Recently Dead Tanoak. However, based on visual interpretation, it does look like some bare ground segments were confused as Recently Dead Tanoak, such as the lower right quadrant and top middle portion of figure 11.

Maximum Likelihood Classification

This section presents the pixel-based 2019 and 2017 MLC classification results and their corresponding accuracy assessments. The two outputs were created using signature files that capture spectral information for each land cover class in the training data. Figure 12 shows a subset of the 2019 MLC results along with the 2019 imagery, while table 3 provides a summary of the errors of commission and omission for the 2019 MLC classification. The complete error matrix is available in Appendix B. The overall accuracy of the 2019 MLC results, 69%, is significantly lower than the SVM results, which had an overall accuracy of 85%. It should be noted, however, that the total accuracies are negatively impacted by the misclassification of certain land cover classes that are of no interest to land managers in this context, such as buildings, roads, and bare ground.

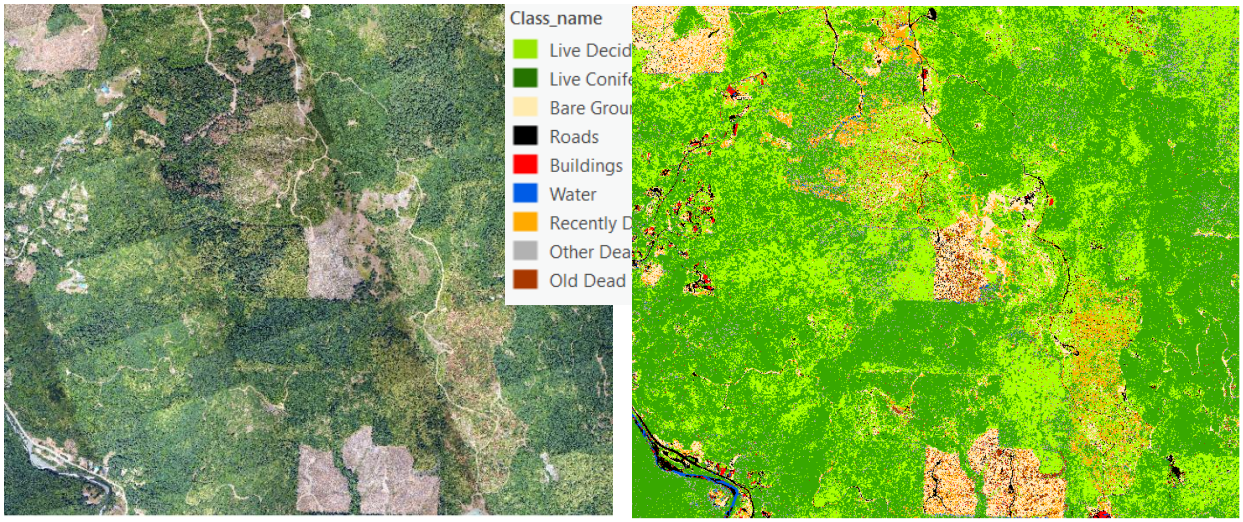

Figure 12: 2019 Image (left) and the Maximum Likelihood Classification result (right).

Table 3: Errors summarized for each of the classes for the 2019 MLC classification.

MLC 2019 subset	Error of Omission (%)	Error of Commission (%)
Live Deciduous	8	0
Live Coniferous	10	10
Bare Ground	36	56
Roads	6	44
Buildings	70	57
Water	0	0
Recently Dead Tanoak	23	14
Other Dead	79	0
Old Dead Tanoak	7	54
Total Accuracy (%)		69

The 2017 MLC results were created using the same signature file that was applied to the 2019 image in order to test the suitability of having one master training dataset instead of creating a separate training dataset for every year, which is time consuming and a requirement for the SVM classification. Figure 13 shows the image mosaic and classification results for the 2017 MLC iteration, and table 4 shows the summarized errors of omission and commission for those results. The total accuracy of the 2017 MLC classification is very similar to the 2019 results, and some of the same classes have high rates of error (e.g., buildings and bare ground). The error matrix (see Appendix B) indicates that the three dead tree classes were primarily confused with bare ground.

Like the SVM outputs, there are some areas where Recently Dead Tanoak was predicted accurately in both the 2017 and 2019 MLC outputs, and others where bare ground was misclassified as Recently Dead Tanoak. In figure 12, these misclassified areas of Recently Dead Tanoak (orange) are predominantly in

the lower right quadrant of the image. In figure 13, these misclassified areas are largely in the upper middle and upper left of the image.

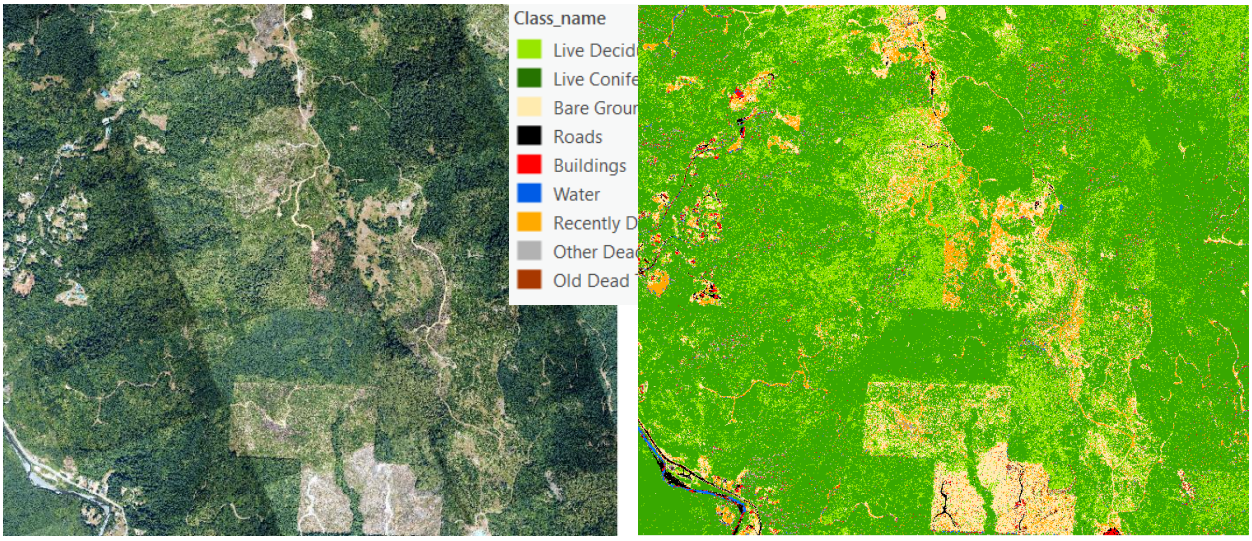

Figure 13: 2017 Image Mosaic (left), MLC Classification Result (right)

Table 4: Errors summarized for each of the classes for the 2017 MLC classification.

MLC 2017 subset	Error of Omission (%)	Error of Commission (%)
Live Deciduous	8	0
Live Coniferous	0	33
Bare Ground	30	65
Roads	40	25
Buildings	33	0
Water	0	0
Recently Dead Tanoak	28	19
Other Dead	50	38
Old Dead Tanoak	55	29
Total Accuracy (%)		72

Maximum Entropy (MaxEnt) Classification

The purpose of exploring the MaxEnt classification was to test if this approach would be more time-efficient than the MLC or SVM approaches. As with the other tests, the 2019 data were used in order to maintain consistency through all the classification methods. Figure 14 shows the MaxEnt output where Recently Dead Tanoak was the target class. The result is a classified image showing probability values, where warmer colors (reds, oranges, and yellows) indicate a higher probability that the pixel belongs to the class that is being predicted.

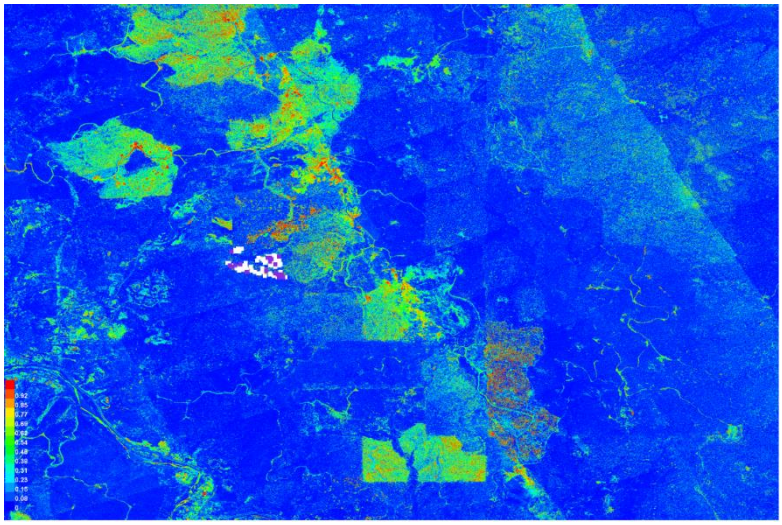

Figure 14: 2019 MaxEnt output for the Recently Dead Tanoak class, where the warmer (redder) the color, the more likely it is to be Recently Dead Tanoak.

Figure 15 shows the results from a second MaxEnt test, in which the target class was the Other Dead class, which represents grey dead trees that are not tanoak. One issue that is apparent in each of the MaxEnt results is that the general area that overlaps with the training data points are excluded from the output probability maps. Only a qualitative visual assessment, not a formal accuracy assessment, was performed on this result.

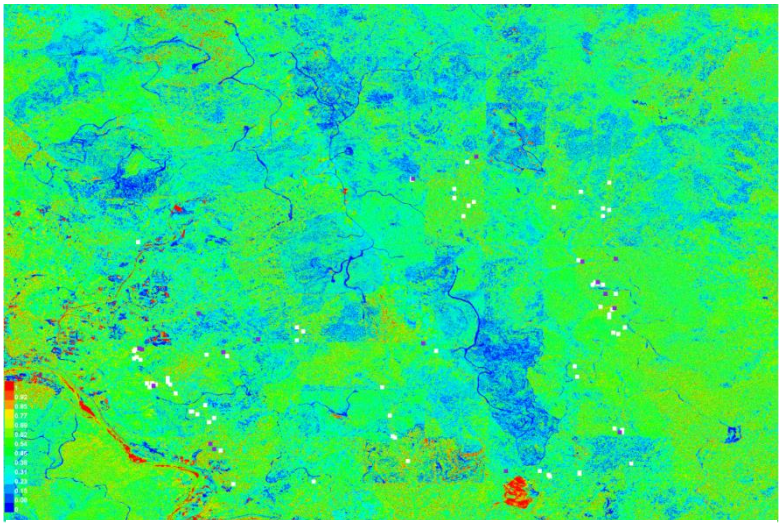

Figure 15: 2019 MaxEnt output for the Other Dead Trees class, where the warmer (redder) the color, the more likely it is the Other Dead Tree class.

The output for the Other Dead class has generally higher probability values (more green) than the Recently Dead Tanoak values, which were more blue, and that is likely because the spectral values associated with grey dead trees are more common throughout the study area than the reddish-brown signature of Recently Dead Tanoaks.

Discussion and Next Steps

Structure from Motion

At the outset of this project, SfM seemed like a promising approach to find innovative ways to identify symptoms of SOD, and potentially even identify early onset symptoms by detecting slight changes in canopy structure. Unfortunately, the quality of the SfM-derived 3D point cloud was compromised by the limited sidelap and endlap of the aerial imagery. The point cloud and resulting DSM were riddled with gaps, and the canopy surface had limited structural detail that could facilitate the cross-year comparison of DSMs or CHMs. Furthermore, at the time of the project, high resolution DEMs were only available for a small portion of the western part of the study area, meaning the quality and resolution of any canopy height data would be adversely affected.

In addition to the complications with the SfM-derived data in this specific project, there may be general issues with this approach: the consistently high canopy cover and the similar canopy height exhibited in tanoak stands could prove detrimental to the production of high quality canopy data (e.g., CHM) that would enable a tree-by-tree analysis (e.g., individual tree segmentation). This could potentially be the case even if the aerial imagery is collected with the right endlap and sidelap specifications for SfM workflows, but we can't be sure. Because of all these factors, the SfM derived data did not prove useful for SOD identification.

Supervised Classifications

Each supervised classification that was tested encountered similar issues: bare ground and grey dead tree classes were consistently confused with one another due to their similar spectral characteristics, and the separation of grey dead tanoak from Other Dead grey trees proved inaccurate. The classification algorithm that performed the best was SVM, which had an overall accuracy of 85%. This approach, however, also takes the most amount of effort to run for every year because it requires a new training dataset and new segments for each annual mosaic. Moreover, it still has relatively high error rates for some of the dead tree classes. Any use of this classified data would still require some image interpretation to identify areas where dead tanoak and Recently Dead Tanoak were classified incorrectly.

The outputs from the MLC approach were not as promising as those from SVM, as the 2017 and 2019 overall accuracies were 72% and 69%, respectively. As expected, the old dead tanoak and Other Dead classes were consistently confused with one another, and their errors of commission and omission reflect this. The Recently Dead Tanoak class was mapped relatively accurately for both 2017 and 2019, and the most common class that it is confused with is bare ground. A visual interpretation of some areas, however, clearly showed that Recently Dead Tanoak was over predicted in areas of bare ground, particularly in areas where the soil looked spectrally similar to the reddish-brown tanoak. Although the overall accuracy of the MLC results were not as high as we would have liked, the simplicity and cross-year applicability of the signature files derived from the training data still make MLC an attractive option, especially if the output will be used to guide a more manual image interpretation approach.

The MaxEnt approach seemed appealing because it is not a classification approach that requires training data for all the different land cover types in the study area. It instead ingests a training dataset for a

single target class and produces a probability map. But the lack of intuitive input parameters and the need to convert all of the high-resolution images to ASCII format is cumbersome. Moreover, the probability map outputs would require further post-processing to identify a probability threshold that would filter out most of the pixels that don't belong to the target class.

Recommendations and Next Steps

While the SfM workflow was generally unsuccessful for this project, it could potentially be successful in the future if aerial imagery is collected with the recommended 80% endlap, 60% sidelap specifications. Individual tree segmentation may still not be feasible for tanoak stands, however, due to the tightly knit canopies and the apparent even age of tanoaks. Also, a 2019 acquisition of lidar data will complete lidar coverage in the study area, meaning that a high resolution DTM will be available for future workflow tests (a necessary product to produce CHMs). Although we cannot be certain that high quality SfM-derived point clouds and subsequent raster products would aid in the monitoring of early onset SOD symptoms, we do think that this would be worth exploring in a future project. At the very least, high quality DEM and CHM data could facilitate the creation of a relatively accurate forest/non-forest mask that could be used to remove false positives in the classifications where bare earth or road pixels are classified as dead trees.

The supervised classification of dead tanoak proved to be difficult due to the frequent misclassification of dead trees as bare earth and vice-versa. The differentiation of dead tanoak from Other Dead trees was also problematic, as grey dead tanoak are spectrally similar to dead Douglas firs. Because of the obvious errors in the classification results, they cannot be used as a final product to quantify SOD coverage on a year to year basis. The results can, however, aid in image interpretation and the digitization of dead tanoak, especially since bare earth classified as dead trees/tanoak is easy to ignore during image interpretation. Furthermore, the potential production of the aforementioned high-resolution tree/non-tree mask for this study area could greatly improve classification results.

Deliverables

The deliverables for this project include a set of exercises that provide step-by-step instructions for (1) clipping individual images and creating new mosaics, (2a) creating training data and performing MLC, (2b) segmenting imagery and performing SVM, and (3) producing error matrices for an accuracy assessment. These exercises, the python script as well as sample imagery and training datasets are available here: https://fsapps.nwcg.gov/gtac/CourseDownloads/GeoTASC/FY19/SOD/. All the classification results and training data presented in this report will also be shared with cooperators. In addition, depending on the usefulness of the material to cooperators, we may provide results from earlier classification results not presented in this report, as well as the raster and point cloud outputs from the SfM workflow.

References

Burnett, J.; 2017. Environmental Remote Sensing with Unmanned Aircraft Systems. Oregon State University.

Garbelotto, M.; Svihra, P.; Rizzo, D. 2001. New pests and diseases: Sudden oak death syndrome fells 3 oak species. California Agriculture. 55(1):9-19.

Goheen, E.M.; Hansen, E.M.; Kanaskie, A.; McWilliams, M.G.; Osterbauer, N.; Sutton, W. 2002. Sudden oak death caused by Phytophthora ramorum in Oregon. Plant disease. *86*(4): 441-441.

Goheen, E.M.; Kanaskie, A.; McWilliams, M.; Hansen, E.; Sutton, W.; Osterbauer, N. 2006. Surveying and monitoring sudden oak death in southwest Oregon forests. Proceedings of the sudden oak death second science symposium: the state of our knowledge. Gen. Tech. Rep. PSW-GTR-196. Albany, CA: Pacific Southwest Research Station, Forest Service, US Department of Agriculture: 413-415 (Vol. 196).

Goheen, E.M.; Kanaskie, A.; Navarro, S.; Hansen, E. 2017. Sudden oak death management in Oregon tanoak forests. Forest Phytophthoras. 7(1):45-53.

Grünwald, N.J.; Garbelotto, M.; Goss, E.M.; Heungens, K. Prospero, S. 2012. Emergence of the sudden oak death pathogen Phytophthora ramorum. Trends in microbiology. 20(3):131-138.

Hansen, E.; Reeser, P.; Sutton, W.; Kanaskie, A.; Navarro, S.; Goheen, E.M. 2019. Efficacy of local eradication treatments against the sudden oak death epidemic in Oregon tanoak forests. Forest Pathology. P. e12530.

Oommen, T., Misra, D., Twarakavi, N.K., Prakash, A., Sahoo, B. and Bandopadhyay, S., 2008. An objective analysis of support vector machine based classification for remote sensing. Mathematical geosciences, 40(4), pp.409-424.

Panagiotidis, D.; Abdollahnejad, A; Surový, P.; Chiteculo, V. 2017. Determining tree height and crown diameter from high-resolution UAV imagery. International journal of remote sensing. 38(8-10): 2392-2410.

Phillips, Steven J., Robert P. Anderson, Miroslav Dudík, Robert E. Schapire, and Mary E. Blair. "Opening the black box: An open-source release of Maxent." Ecography 40, no. 7 (2017): 887-893.

Verhoeven, G. 2011. Taking computer vision aloft–archaeological three-dimensional reconstructions from aerial photographs with photoscan. Archaeological prospection. 18(1): 67-73.

Wallace, L., Lucieer, A., Malenovský, Z., Turner, D. and Vopěnka, P., 2016. Assessment of forest structure using two UAV techniques: A comparison of airborne laser scanning and structure from motion (SfM) point clouds. Forests. 7(3): 62.

Webb, J.; Fisk, H. 2017. Aerial image acquisition considerations for phodar forestry applications. GTAC-10124-Brief 1. Salt Lake City, UT: U.S. Department of Agriculture, Forest Service, Geospatial Technology and Applications Center. 10 p.

Westoby, M.J.; Brasington, J.; Glasser, N.F.; Hambrey, M.J.; Reynolds, J.M. 2012. 'Structure-from-Motion' photogrammetry: A low-cost, effective tool for geoscience applications. Geomorphology. 179: 300-314.

Appendix A

SVM Segmentation testing

This section presents the results from the SVM segmentation results, which were performed to see which segmentation parameters produced the best results. Five different sets of parameters were tested with the 2019 imagery. The number of training data points collected for the earlier classification iterations for this project are greater than the total points used in the classifications presented in the Results section. This is because our classification scheme evolved to incorporate different dead tree classes, and we had a limited capacity to collect more training points for each of those new classes.

2019 SVM:

1. Segmentation parameters- spectral weight: 20, spatial weight: 15, minimum segment size: 50px.

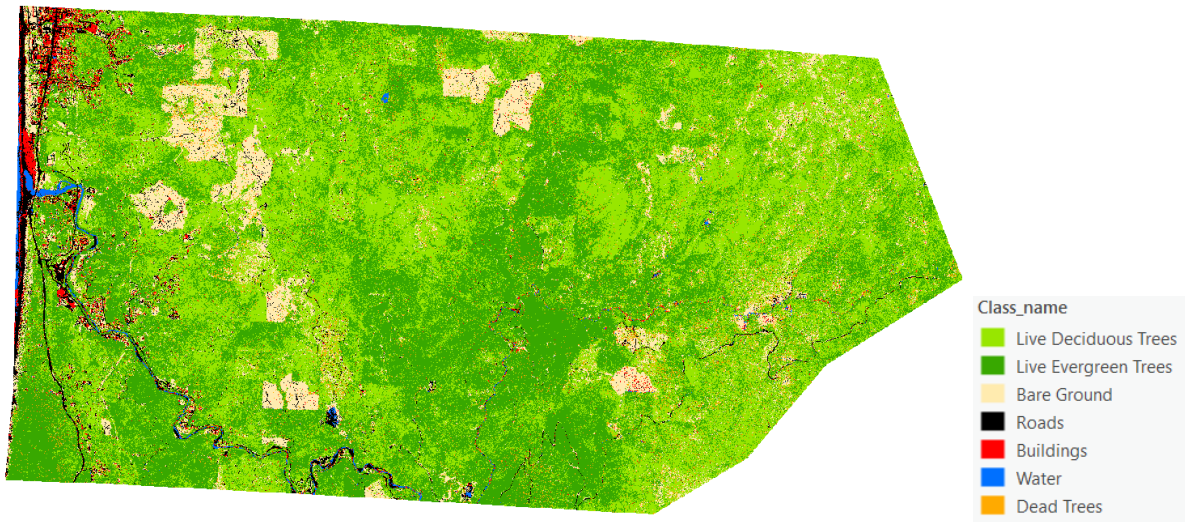

SVM 201550	Classified Data										
Reference Data		Live Deciduous	Live Evergreen	Bare Ground	Road	Buildings	Water	Dead Trees	Total	Error of Omission (%)	Producer's Accuracy (%)
	Live Deciduous	102	12	1	0	0	0	1	116	12	88
	Live Evergreen	5	104	1	0	0	0	0	110	5	95
	Bare Ground	3	0	62	5	2	2	0	74	16	84
	Road	2	0	6	139	18	1	0	166	16	84
	Buildings	0	0	2	17	171	1	3	194	12	88
	Water	0	0	0	4	0	95	1	100	5	95
	Dead Trees	2	0	2	0	5	0	94	103	9	91
	Total	114	116	74	165	196	99	99	863		
	Error of Commission (%)	11	10	16	16	13	4	5		89	Total Accuracy (%)
	User's Accuracy (%)	89	90	84	84	87	96	95			

2. Segmentation parameters- spectral weight: 20, spatial weight: 15, minimum segment size: 100px.

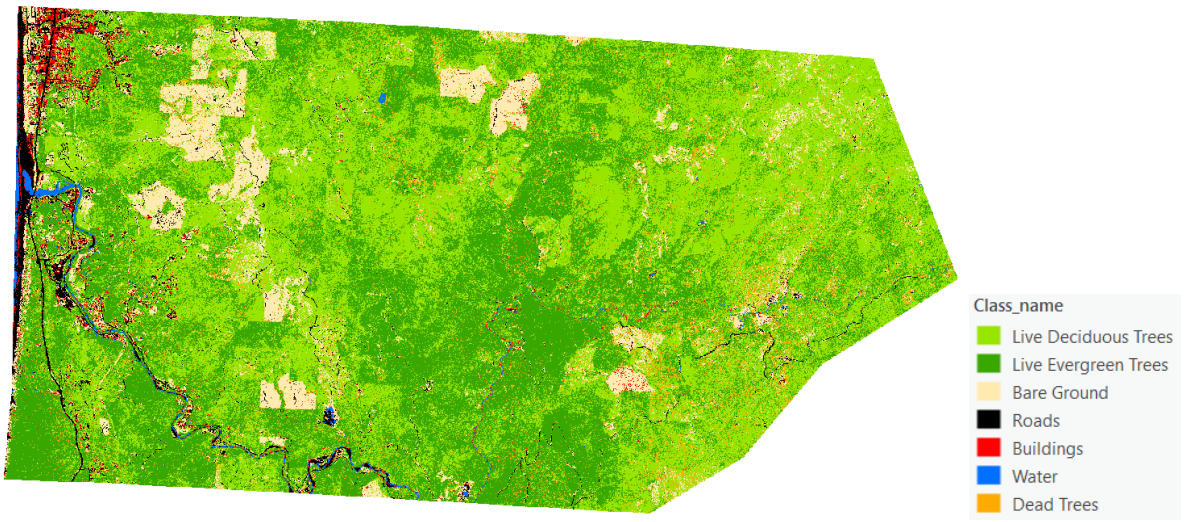

SVM_2015100		Classified Data									
		Live Deciduous	Live Evergreen	Bare Ground	Road	Buildings	Water	Dead Trees	Total	Error of Omission (%)	Producer's Accuracy (%)
Reference Data	Live Deciduous	105	10	0	0	0	0	1	116	9	91
	Live Evergreen	7	101	0	0	0	0	2	110	8	92
	Bare Ground	3	2	66	0	0	2	1	74	11	89
	Road	1	0	3	141	21	0	0	166	15	85
	Buildings	0	0	5	15	172	1	1	194	11	89
	Water	0	1	0	1	2	96	0	100	4	96
	Dead Trees	0	5	3	0	2	0	93	103	10	90
	Total	116	119	77	157	197	99	98	863		
	Error of Commission (%)	9	15	14	10	13	3	5		90	Total Accuracy (%)
	User's Accuracy (%)	91	85	86	90	87	97	95			

3. Segmentation parameters- spectral weight: 20, spatial weight: 15, minimum segment size: 150px.

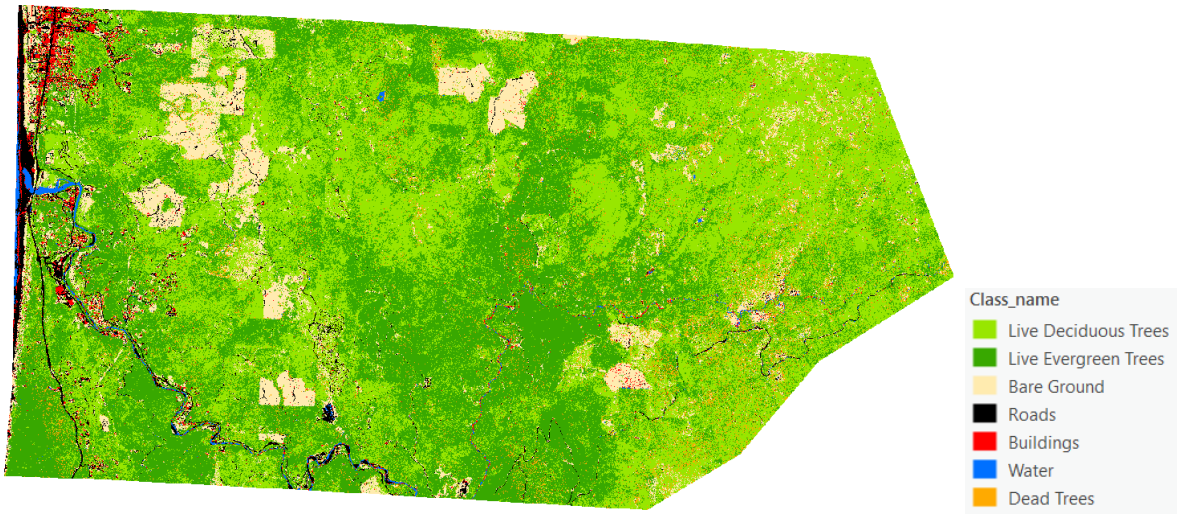

SVM_2015150		Classified Data									
		Live Deciduous	Live Evergreen	Bare Ground	Road	Buildings	Water	Dead Trees	Total	Error of Omission (%)	Producer's Accuracy (%)
Reference Data	Live Deciduous	107	8	1	0	0	0	0	116	8	92
	Live Evergreen	2	107	0	0	0	0	1	110	3	97
	Bare Ground	1	0	69	1	1	1	1	74	7	93
	Road	0	0	2	146	16	2	0	166	12	88
	Buildings	0	0	3	11	177	2	1	194	9	91
	Water	0	0	0	4	2	93	1	100	7	93
	Dead Trees	3	5	1	0	2	0	92	103	11	89
	Total	113	120	76	162	198	98	96	863		
	Error of Commission (%)	5	11	9	10	11	5	4		92	Total Accuracy (%)
	User's Accuracy (%)	95	89	91	90	89	95	96			

4. Segmentation parameters- spectral weight: 20, spatial weight: 15, minimum segment size: 200px.

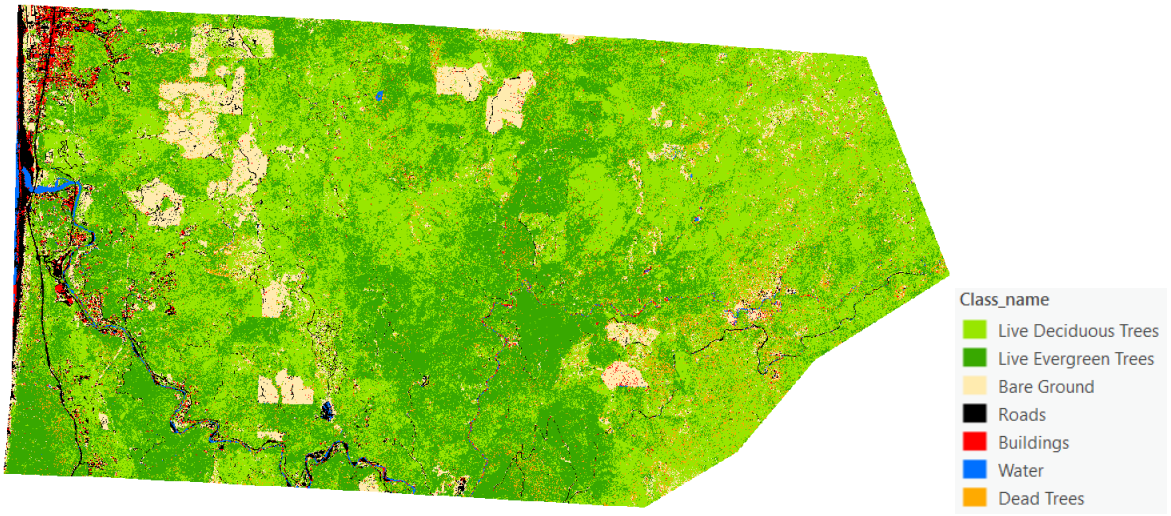

SVM_2015200		Classified Data									
		Live Deciduous	Live Evergreen	Bare Ground	Road	Buildings	Water	Dead Trees	Total	Error of Omission (%)	Producer's Accuracy (%)
Reference Data	Live Deciduous	111	5	0	0	0	0	0	116	4	96
	Live Evergreen	3	106	0	0	0	0	1	110	4	96
	Bare Ground	1	0	69	1	1	1	1	74	7	93
	Road	0	0	0	147	18	1	0	166	11	89
	Buildings	0	0	3	10	176	3	2	194	9	91
	Water	0	0	0	4	0	95	1	100	5	95
	Dead Trees	0	2	0	0	2	0	97	101	4	96
	Total	115	113	72	162	197	100	102	861		
	Error of Commission (%)	3	6	4	9	11	5	5		93	Total Accuracy (%)
	User's Accuracy (%)	97	94	96	91	89	95	95			

5. Segmentation parameters- spectral weight: 20, spatial weight: 20, minimum segment size: 50px.

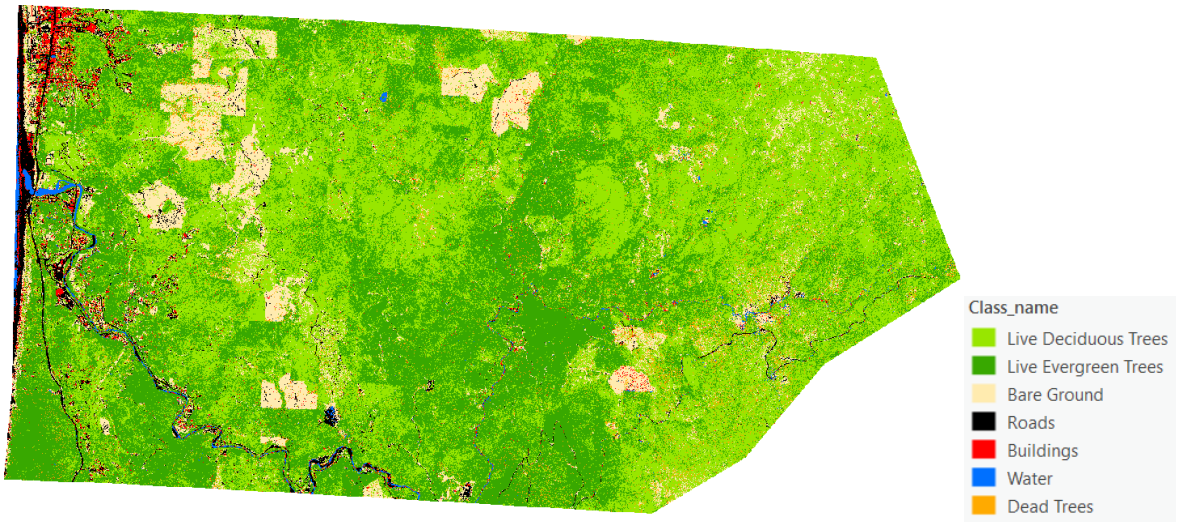

SVM_202050	Classified Data										
		Live Deciduous	Live Evergreen	Bare Ground	Road	Buildings	Water	Dead Trees	Total	Error of Omission (%)	Producer's Accuracy (%)
Reference Data	Live Deciduous	109	5	0	0	1	0	1	116	6	94
	Live Evergreen	8	102	0	0	0	0	0	110	7	93
	Bare Ground	2	0	65	2	1	2	2	74	12	88
	Road	0	0	2	145	19	0	0	166	13	87
	Buildings	0	0	1	18	169	1	5	194	13	87
	Water	0	0	0	2	3	94	1	100	6	94
	Dead Trees	3	2	2	0	5	0	91	103	12	88
	Total	122	109	70	167	198	97	100	863		
	Error of Commission (%)	11	6	7	13	15	3	9		90	Total Accuracy (%)
	User's Accuracy (%)	89	94	93	87	85	97	91			

Appendix B

This Appendix provides the detailed error matrices that were summarized in the Results section.

SVM 2019		Classified Data											
		Live Deciduous	Live Coniferous	Bare Ground	Roads	Buildings	Water	Recently Dead Tanoak	Other Dead Trees	Old Dead Tanoak	Total	Error of Omission (%)	Producer's Accuracy (%)
Reference Data	Live Deciduous	12	0	0	0	0	0	0	0	1	13	8	92
	Live Coniferous	0	9	0	0	0	0	0	1	0	10	10	90
	Bare Ground	0	0	10	1	0	0	0	0	0	11	9	91
	Roads	0	0	0	15	1	0	0	0	0	16	6	94
	Buildings	0	1	2	3	4	0	0	0	0	10	60	40
	Water	0	0	0	0	0	9	0	0	0	9	0	100
	Recently Dead Tanoak	0	0	1	0	0	0	36	2	0	39	8	92
	Other Dead Trees	0	1	2	0	0	0	0	22	3	28	21	79
	Old Dead Tanoak	0	0	0	0	1	0	1	2	10	14	29	71
	Total	12	11	15	19	6	9	37	27	14	150		
	Error of Commission (%)	0	18	33	21	33	0	3	19	29		85	Total Accuracy (%)
	User's Accuracy (%)	100	82	67	79	67	100	97	81	71			

MLC 2019		Classified Data											
		Live Deciduous	Live Coniferous	Bare Ground	Roads	Buildings	Water	Recently Dead Tanoak	Other Dead Trees	Old Dead Tanoak	Total	Error of Omission (%)	Producer's Accuracy (%)
Reference Data	Live Deciduous	12	0	0	0	0	0	1	0	0	13	8	92
	Live Coniferous	0	9	0	0	0	0	0	0	1	10	10	90
	Bare Ground	0	0	7	1	1	0	2	0	0	11	36	64
	Roads	0	0	0	15	0	0	0	0	1	16	6	94
	Buildings	0	1	1	5	3	0	0	0	0	10	70	30
	Water	0	0	0	0	0	9	0	0	0	9	0	100
	Recently Dead Tanoak	0	0	8	0	0	0	30	0	1	39	23	77
	Other Dead Trees	0	0	0	6	3	0	1	6	12	28	79	21
	Old Dead Tanoak	0	0	0	0	0	0	1	0	13	14	7	93
	Total	12	10	16	27	7	9	35	6	28	150		
	Error of Commission (%)	0	10	56	44	57	0	14	0	54		69	Total Accuracy (%)
	User's Accuracy (%)	100	90	44	56	43	100	86	100	46			

MLC 2017		Classified Data											
Reference Data		Live Deciduous	Live Coniferous	Bare Ground	Roads	Buildings	Water	Recently Dead Tanoak	Other Dead Trees	Old Dead Tanoak	Total	Error of Omission (%)	Producer's Accuracy (%)
	Live Deciduous	12	1	0	0	0	0	0	0	0	13	8	92
	Live Coniferous	0	6	0	0	0	0	0	0	0	6	0	100
	Bare Ground	0	0	7	0	0	0	3	0	0	10	30	70
	Roads	0	0	2	3	0	0	0	0	0	5	40	60
	Buildings	0	0	0	1	6	0	0	0	2	9	33	67
	Water	0	0	0	0	0	8	0	0	0	8	0	100
	Recently Dead Tanoak	0	0	4	0	0	0	13	1	0	18	28	72
	Other Dead Trees	0	1	4	0	0	0	0	5	0	10	50	50
	Old Dead Tanoak	0	1	3	0	0	0	0	2	5	11	55	45
	Total	12	9	20	4	6	8	16	8	7	90		
	Error of Commission (%)	0	33	65	25	0	0	19	38	29		72	Total Accuracy
	User's Accuracy (%)	100	67	35	75	100	100	81	63	71			